Structure and Concentration Decay in Supercritical Plane Hydrogen Jet

D. Makarov* and V. Molkov

Hydrogen Safety Engineering and Research (HySAFER) Centre, University of Ulster Newtownabbey, Co. Antrim, BT37 0QB, United Kingdom

*Corresponding author: dv.makarov@ulster.ac.uk

The structure, axial concentration decay, and formation of flammable hydrogen-air mixture are studied numerically for a case of hydrogen release from a round nozzle and a plane nozzle with aspect ratio 200. Simulations of the underexpanded hydrogen jet structure for both circular and plane nozzles were conducted using the computational fluid dynamics in two stages: firstly from the nozzle across the shocks' structure, and secondly downstream from the Mach disk to the far field. The results confirmed the phenomenon of "switching" axes known for plane jets of finite aspect ratio: the faster mixing in the plane of a minor axis makes the jet in this plane wider than in the plane of a major axis. The faster hydrogen-air mixing takes place only in the near field close to the nozzle. Downstream the plane nozzle jet structure tends to reproduce that of the axisymmetric jet. In the far field both plane and round nozzle jets resemble the similarity law for axial concentration decay in round jets.

Keywords: hydrogen safety, underexpanded jet, plane nozzle, axial concentration decay.

1. Introduction

As hydrogen and fuel cell technologies, systems, and infrastructure develop, the use of high-pressure hydrogen storage becomes inevitable. The safety distances around these storage and infrastructure are most likely to be determined based on the location of the lower flammability limit (LFL) in an accident scenario. This causes immense interest to the hydrogen concentration decay in jets, including plane jet which can be considered as a model of a crack. The purpose of this paper is to study to what degree mixing in a plane jet may be intensified and if a plane jet may provide a shorter distance to LFL 4% of hydrogen by volume compared to a round jet with the same mass flow rate.

First analytical studies of laminar subsonic constant density jets in absence of buoyancy forces date back to 1920s. Schlichting studied an axisymmetric and plane laminar jets issued into a semi-infinite space [1]. The plane jet solution was subsequently improved by Bickley [2]. Both are exact solutions of Prandtl's boundary layer equations and may be found in the classical textbook [3]. The results show that compare to the infinitely long plane jet the axysimmetric laminar jet has larger entrainment potential (entrains more surrounding fluid) and the infinite plane jet is less effective in mixing with the surrounding quiescent fluid. Thus, theoretical studies indicate that the axial concentration decay in the plane jet of the same width as round jet diameter could be slower compared to the round jet.

Qualitatively similar results were obtained for the turbulent jets [3]: based on observation that the turbulent mixing length is proportional to the jet width and, as a result, the jet width for both

circular and plane jets is proportional to the distance from the nozzle x (though with different proportionality coefficients), the decay of the centre-line velocity V in a momentum-dominated turbulent round jet is proportional to x^{-1}, while the same for the plane jet is proportional to $x^{-1/2}$, which means that the round jet entrainment rate is higher than that of the infinitely long plane jet. Comprehensive overview of experimental data available for velocity and species concentrations in momentum- and buoyancy-dominated incompressible turbulent jets is given in [4] for both plane and axisymmetric configurations and for jets with different densities of mixing gases.

Analytical solution for compressible plane and round turbulent jets was obtained by Crane and Pack [5], though based on a number of simplifying assumptions. It was found that for a plane jet the compressibility effect decreases width of mixing region for laminar jets and increases it for the turbulent jet. For axially symmetric jets the compressibility resulted in narrower velocity profile as the speed rose for both laminar and turbulent flows. This result was confirmed experimentally by Maydew and Reed [6] for Mach numbers up to M=1.96. Later on Crane and Pack developed an analytical solution for a plane jet of gas issued into another gas [7]. There are different engineering approaches, e.g. [8, 9], which allow to extend incompressible axysimmetric jet correlations [4] to compressible underexpanded jets. However, the approaches are not applicable to the underexpanded plane jets.

Jet from a plane nozzle of a finite aspect ratio has attracted attention as capable to provide more intensive momentum and concentration exchange due to a larger interface area for viscous mixing compare to an axisymmetric jet of the same mass flow rate. A series of experiments with incompressible, subsonic compressible and chocked underexpanded jets from a rectangular nozzle of the size $L \times D$=50×3 mm (aspect ratio 16.7) was conducted at Stanford University. The incompressible flow results were reported by Krothapalli et al. [10], the effect of the exit Mach number of a subsonic compressible jet was given in [11], and underexpanded plane jet results are described in [12]. Mean velocity measurements revealed that the incompressible jet structure consists of three regions: a potential core region, a two-dimensional-type region, and an axisymmetric-type region, where velocity decays close to that in axisymmetric jet [10]. It was found that in the two-dimensional type region the jet spreads in the minor axis plane faster compare to that in the major axis plane. The subsonic compressible jet was found to behave similar to the incompressible jet [11]. Underexpanded choked flow studies [12] were conducted using the pressure ratio up to 5.8, which corresponds to Mach numbers up to 1.8. The spreading rate in the minor axis was even higher than for incompressible flow, so that one can think of "switch" of axes: the major axis becomes the minor one, and vice versa. The same dynamics of the jet structure, i.e. transition from initially two-dimensional jet to axisymmetric one downstream,was found for the underexpanded jet [12]. The authors suggested that the two-dimensionality of a plane jet would be preserved the longer downstream the higher pressure ratio.

Similar research, but with aspect ratio of elliptic and rectangular nozzles equal to 3.0, was performed in [13] using cold and hot gas tests. The pressure ratio for the underexpanded cold tests was equal to 3.4 (Mach number 1.5) and 6.4 for the hot gas tests. The authors argued that the elliptic nozzle provided slightly faster mixing than a rectangular nozzle, though the flow was studied on the distance of 30 equivalent nozzle diameters only. This study was later extended to pressure ratio 15 [14], though was aimed at near-field pressure fluctuations interaction with the spread rate of the jet and remained limited to 30 equivalent diameters. Further studies of underexpanded jet flows from oval nozzles were performed in [15]. It was confirmed that the pressure ratio has a significant effect on the jet spreading in the minor axis and the axis

"switching" strongly depends on both pressure and aspect ratio of the nozzle, though the study was limited to pressure ratio 20.3 and near nozzle area. Numerical simulation of the jet flow from a rectangular nozzle of aspect ratio 8 and pressure ratio 50 was performed in [16], but was limited to the study of the near-nozzle shock structure only.

The potential of a plane nozzle jet to provide more effective mixing compare to axisymmetric jets is of immediate interest for hydrogen safety engineering. The authors are not aware of experimental measurements of hydrogen concentrations in plane nozzle jets covering the range of characteristic pressure ratios 350-700, and correlations similar to [4] which are applicable to plane nozzles of finite aspect ratio. The present study will concentrate on computational fluid dynamics (CFD) modelling of a plane nozzle jet of large aspect ratio 200 in order to understand dynamics of plane jet structure with limited aspect ratio, estimate axial hydrogen concentration decay in such a flow, and to quantify the intensification of hydrogen-air mixing.

2. Problem Formulation

The CFD model. The effective diameter approaches similar to [8, 9], allowing to simplify underexpanded jet modelling and to avoid consideration of underexpanded jet shock structure including Mach disk(s), are not applicable to the finite aspect ratio plane jets. Once simplification of the flow structure is not available, numerical simulations should rigorously resolve flow in the nozzle, shock structure, supersonic flow downstream of the Mach disk and further mixing in the subsonic flow area. Discrepancy of scales between the physical nozzle size, where compressible flow solver and Courant-Friedrichs-Lewy condition should be applied, and the distance of jet propagation to LFL, where flow is subsonic and slowly developing, makes modelling of this phenomenon through the whole domain of interest computationally expensive. Instead, two-stage modelling is applied in this study: first we model the flow through the nozzle across Mach disk structure, and then from the Mach disk to the far field, using a quasi-steady solution of the first stage as a boundary condition for the second stage. The similar two-stage strategy was used for the underexpanded axisymmetric jet modelling [17].

The CFD model consists of three-dimensional steady-state Navier-Stokes equations, energy and species conservation equations. The standard k-ε model [18] with full buoyancy effects was adopted for turbulence modelling as a pragmatic and computationally inexpensive choice. The Navier-Stokes equations were solved in a fully compressible form using a coupled explicit solver at the first stage of simulations, while at the second stage the flow was treated as incompressible and a segregated solver was applied. First order upwind discretisation scheme was used at the first stage to avoid numerical instabilities and the third order MUSCL discretisation scheme was used at the second stage. Simulations were conducted using the CFD code FLUENT.

In this study a release through a round nozzle of 1.58 mm diameter was compared with a leak through a plane nozzle of the size $L \times W = 20 \times 0.1$ mm (aspect ratio 200). The hydrogen storage pressure 350 atm was chosen in this study: it is yet characteristic for automotive applications, but has reduced error associated with the use of the ideal gas equation of state as compared to 700 atm. Indeed, hydrogen density according to the ideal gas equation of state at 350 atm is 29.3 kg/m^3, and according to the Abel-Noble equation of state is 23.9 kg/m^3 yielding difference of about 18%.

Round nozzle calculation domain and numerical details. The calculation domains for the round jet simulations are shown in Figure 1. Calculation domain for the fist stage has cylindrical

shape and sizes $L \times D$=0.25×0.16 m. The domain included small high-pressure "vessel" upflow from the nozzle, where hydrogen inflow was modelled. The domain was discretised by 412736 hexahedral control volumes (CV). The round nozzle of 1.58 mm diameter and 5 mm depth was discretised by 20 CVs across its diameter and 16 CVs in depth. The Mach disk was discretised approximately by 50 CVs across its diameter and 40 CVs in length. Zero pressure boundary conditions were used at all boundaries except of hydrogen inflow area, where pressure was set to p=350 atm, hydrogen concentration to y_{H2}=1.0, and temperature to T=293K.

The cylindrical calculation domain for the second stage has size $L \times D$=8.1×4.0 m and was discretised by 178,808 CVs. The conditions on the inflow boundary were approximated from the first stage jet solution using so called "profile" facility of FLUENT software. On all zero pressure boundaries the inflow temperature 293 K, turbulence intensity 10% and turbulence length scale 0.05 m were used for both the first and the second stage of simulations.

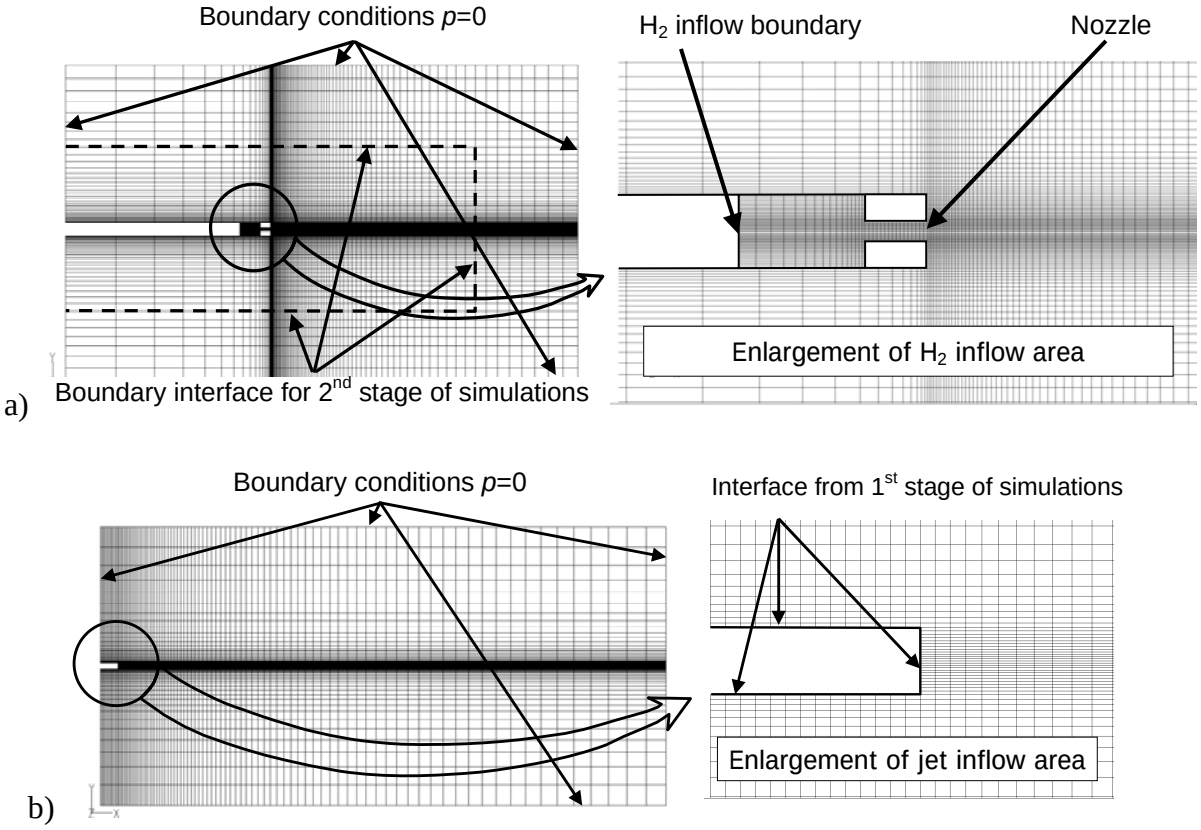

Figure 1. Calculation domain for the round nozzle jet simulations: a) domain for the first stage, b) domain for the second stage.

Plane nozzle calculation domain and numerical details. The plane nozzle is modelled with its major axis directed along a pipe. Calculation domains for the plane nozzle jet simulations are shown in Figure 2. Similar two-stage approach is adopted, though the design of calculation domain utilises symmetry conditions and uses only ¼ of the real physical domain. The calculation domain has sizes $L \times W \times H$=0.125×0.400×0.515 m. Relatively large width of the domain 0.4 m compare to its length 0.125 m is necessary to accommodate the faster hydrogen-air mixing in the plane of the minor axis. The domain was discretised by tetrahedral and hexahedral

CVs, total number is 254,156 CVs. The nozzle has sizes $L \times W$=20×0.1 and depth 5.0 mm, and was discretised by 25 CVs along its half length, 4 CVs along its half width and 16 CVs in depth. Pressure 350 atm, hydrogen concentration 1.0 and temperature 293K were set at the pipe cross section as inflow conditions, zero pressures on the boundaries representing atmosphere and the interface for the second stage of simulations. The domain for the second stage has sizes $L \times W \times H$=2.0×2.0×5.0 m and is discretised by 216,576 CVs. All zero pressure boundaries, representing atmosphere, have the inflow temperature 293 K, turbulence intensity 10% and turbulence length scale 0.05 m similar to that in the round nozzle jet simulations.

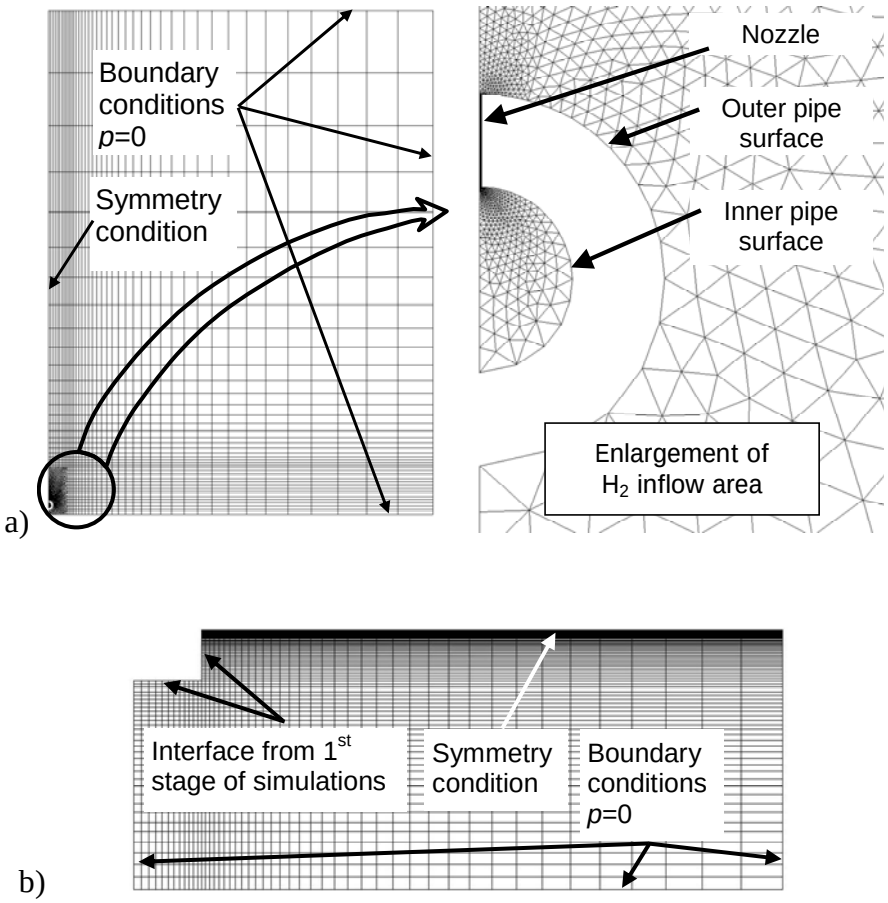

Figure 2. Calculation domain for the plane nozzle jet simulations: a) domain for the first stage, b) domain for the second stage (rotated 90° clockwise).

3. Simulation Results

Hydrogen mass concentration decay obtained in simulations along the jet centre-line for both round and plane jets is shown in Figure 3 in comparison with the similarity law for hydrogen concentration decay in axysimmetric jet, which was developed for incompressible flows in [4] and expanded to compressible flows in [9]:

$$y_{H_2} = 5.4\sqrt{\frac{\rho_N}{\rho_S}}\frac{D}{x}, \qquad (1)$$

where y_{H_2} is hydrogen mass fraction, $\rho_N = 13.0\,kg/m^3$ is density of injected gas in the nozzle according to Abel-Noble equation of state and taking into account pressure losses in the nozzle [19], $\rho_S = 1.20\,kg/m^3$ is density of surrounding air, $D = 1.58\,mm$ is the round nozzle diameter, x is axial distance.

One can see that both plane and round nozzle jets exhibit core regions of jet development, where hydrogen concentration is equal to 1.0. The core region is longer for the round nozzle jet (about 8 cm) compare to the plane nozzle jet (about 3 cm). The plane nozzle jet provides relatively faster mixing than the round nozzle jet in the region x=0.04 – 0.40 m (range of distance to diameter ratios $x/D \approx$25-250). After x=0.40 m, when the axial concentration in the jet is about 50% by volume, the decay of hydrogen concentration for both nozzles is approximately the same, which suggests that the plane nozzle jet becomes close to axysimmetric shape.

From a critical point of view one may be concerned with the higher hydrogen concentration for the plane nozzle jet compare to the round nozzle in the far field (difference is about 12%). Partially this could be explained by 6% higher mass flow rate simulated for the plane nozzle (probably due to discretisation errors) or from the process of boundary profile approximation between the first and second simulation stages.

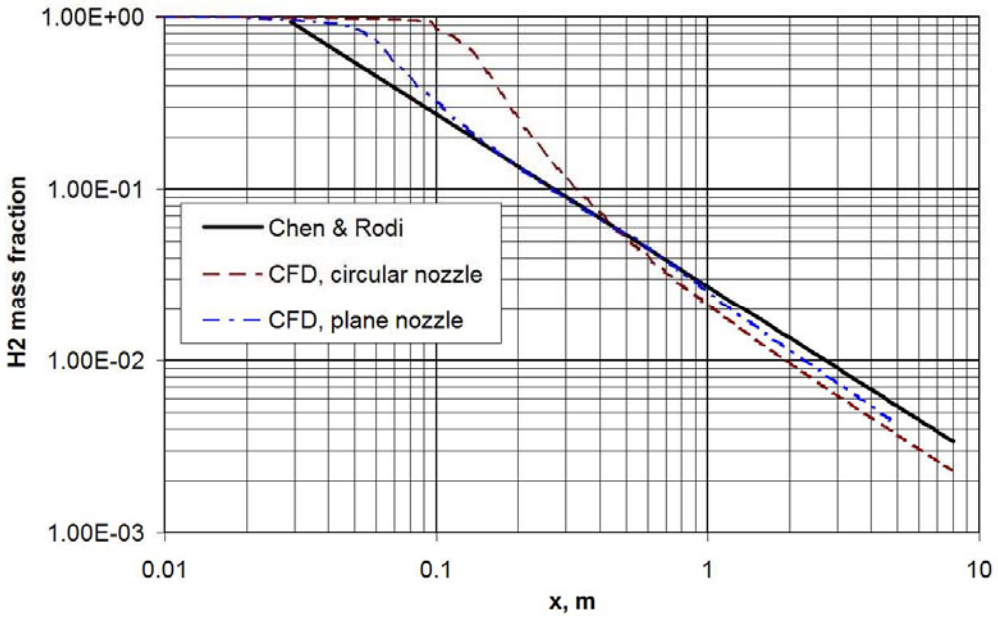

Figure 3. Hydrogen mass fraction distribution along the jet centre-line axis.

It was demonstrated by Saffers and Molkov, see for example overview [20], that the hydrogen-air flames, resulting from round nozzles, have length corresponding to the hydrogen concentration in non-reacting jet between 8% and 16% by volume (best fit line 11%), which corresponds to the mass fraction of hydrogen 0.006 and 0.013. In Figure 3 the jets for both nozzles have qualitatively similar length in this concentration range. However, it was experimentally demonstrated [21] that flame length for a plane nozzle of aspect ratio 12.8 and storage pressure 40 MPa decreases twice compare to the round nozzle. Such a different behavior of non-reacting and reacting jets requires further investigation. This may indicate that the correlation between the

flame length and the hydrogen concentration in a non-reacting jet, obtained in [20] for round nozzle jets, probably may not be automatically extended to nozzles of other shapes.

Qualitatively similar results were obtained for the velocity distribution along the jet centre-line, see Figure 4. They were compared with the correlation for velocity decay in the axisymmetric jet [4]:

$$\frac{V}{V_N} = 6.3\sqrt{\frac{\rho_N}{\rho_S}}\frac{D}{x}, \qquad (2)$$

where V is centre-line velocity, $V_N = 1126\,m/s$ is nozzle velocity according to Abel-Noble equation of state and taking into account pressure losses in the nozzle [19].

Again, the plane nozzle provides faster mixing immediately behind the core region and practically coincides with the round jet velocity distribution in the far field. On the other hand, the centre-line velocity decay for both nozzles is slightly faster than predicted by the correlation (2). Velocity profile reveals location of the Mach disk in simulations: one may see that the Mach disks are located practically at the same distance of about 2.0 cm for both nozzles.

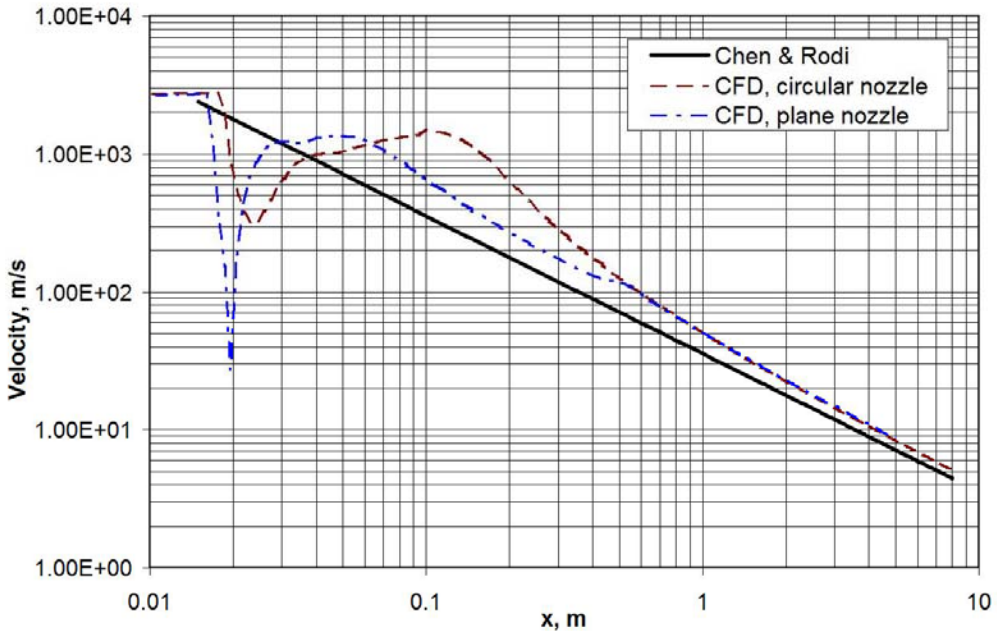

Figure 4. Velocity distribution along the jet centre-line axis.

Comparison of round and plane nozzle jet structures may be seen in Figure 5 and Figure 6, where location of iso-surfaces of 4% and 11% hydrogen volumetric concentrations is shown with the fixed hydrogen concentration distribution profile. The phenomenon of "switching" axes is clearly seen in Figure 6: though the longer side of the plane nozzle is located along the pipe, the wider side of hydrogen-air mixing layer is perpendicular to the pipe. In spite of the large aspect ratio of the plane nozzle L/W=200, the "switch" of axes is already well established at a distance from the nozzle as short as x=0.02 m, which corresponds just to 1 nozzle length.

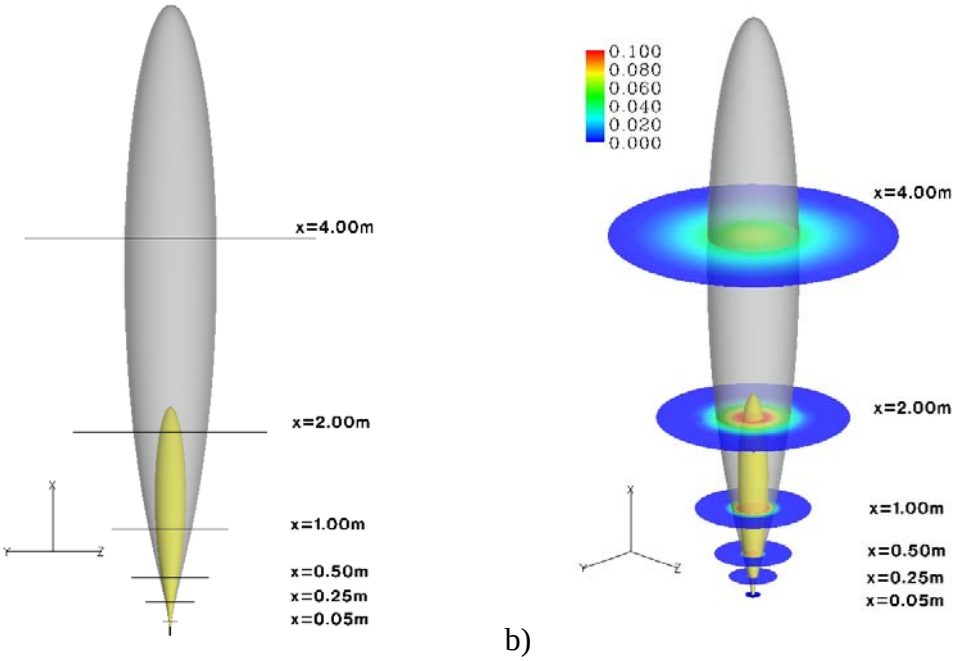

a) b)

Figure 5. Hydrogen iso-surfaces resulting from the round nozzle: a) side view, b) isometric view. Yellow colour – iso-surface 11.0% H_2 vol., grey colour – iso-surface of 4.0% H_2 vol.

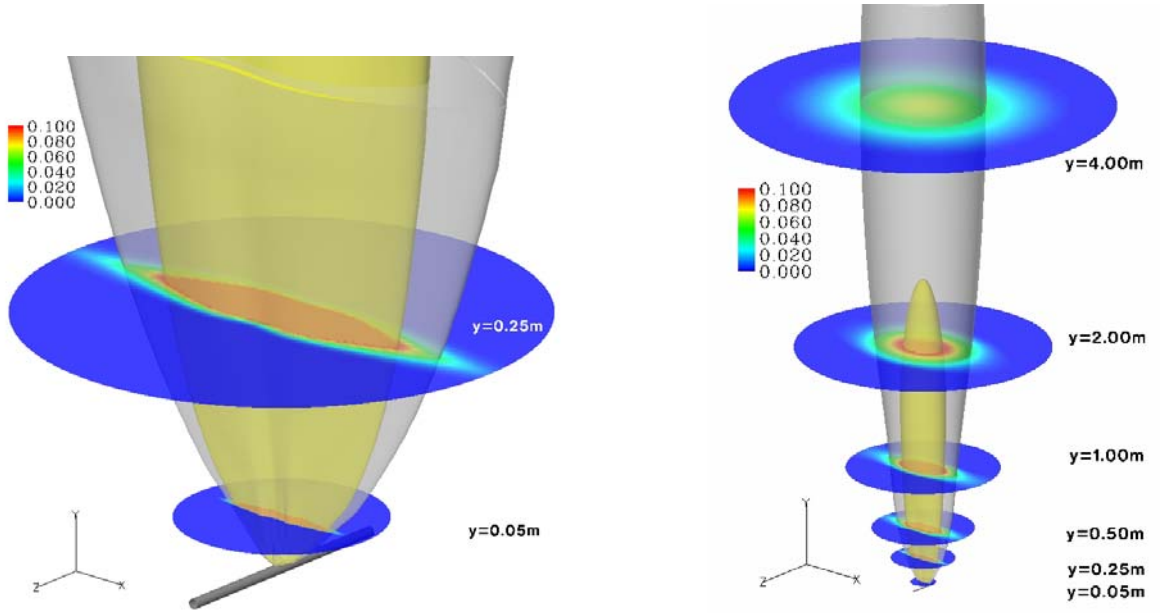

a) b)

Figure 6. Isometric view of hydrogen iso-surfaces resulting from the plane nozzle: a) enlargement close to the pipe, b) general view. Yellow colour – iso-surface 11.0% H_2 vol., grey colour – iso-surface of 4.0% H_2 vol.

Figure 6b confirms that in the far field the plane nozzle jet behavior reproduces axisymmetric jet: effect of axes "switching" is significantly hampered at x=1.0 (when the centre-line concentration

decay of plane nozzle jet coincides with that for the round nozzle jet) and practically absent at x=2.0 m.

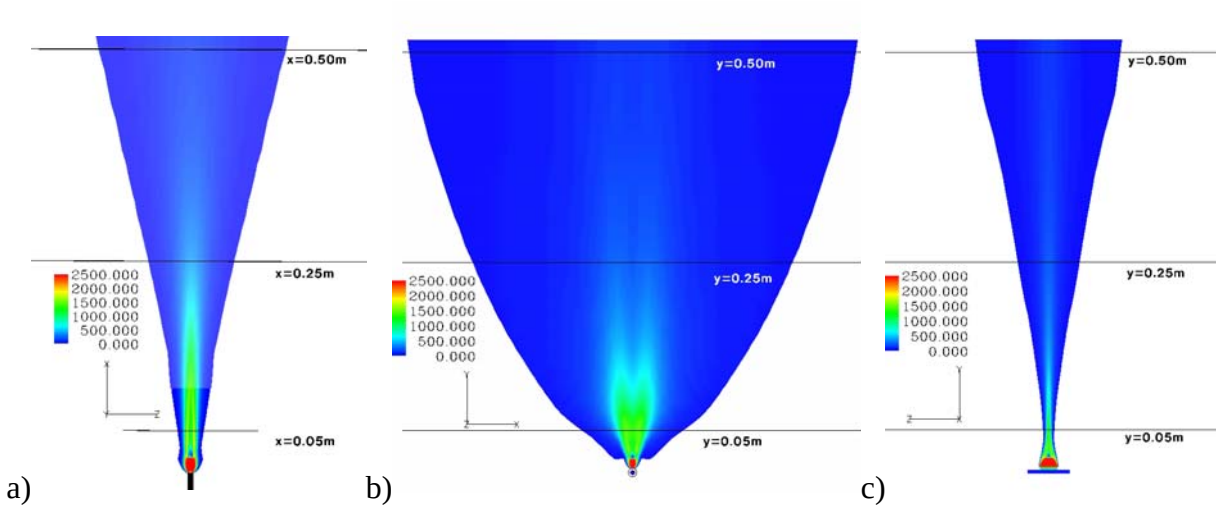

Figure 7. Velocity distribution (limited by 4% H_2 vol.): a) round nozzle, cross-section view, b) plane nozzle, view across the pipe, c) plane nozzle, view along the pipe.

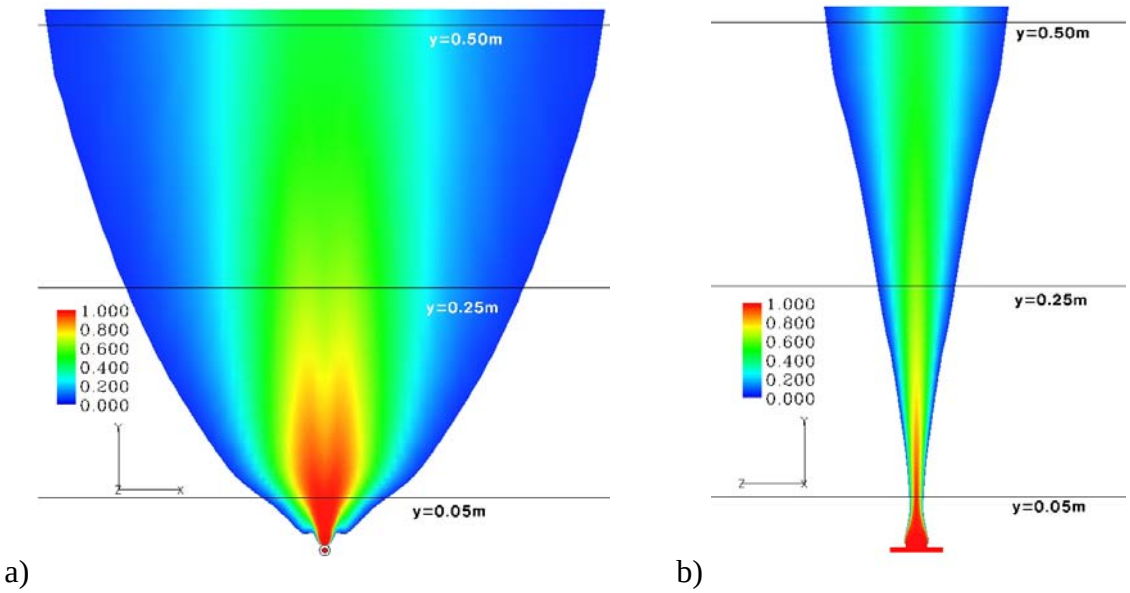

Figure 8. Hydrogen volume fraction distribution in the plane nozzle jet (limited by 4% H_2 vol.): a) across the pipe, b) along the pipe.

Figure 7 shows velocity distribution for the round and plane nozzles in the jet cross sections in the near nozzle field. One may clearly see formation of a wide mixing layer in the plane across the pipe (Figure 7b). Shorter high-speed core region of the plane jet in this cross-section is also noticeable. Mixing layer in the cross-section along the pipe first demonstrates some contraction

("saddle" shape) and then slow growth. Figure 8 shows hydrogen distribution for the plane nozzle jet in the same cross sections. Velocity and concentration fields demonstrate similarity. It is interesting to see that for the plane nozzle the hydrogen velocity and concentration on the centre-line are not necessarily maximum ones. In fact, the maximum velocity and maximum concentration are shifted off centre-line at distances x=0.15-0.30 m. Thus, at x=0.15 m maximum hydrogen mass fraction is 0.23, while on the centre line it is 0.18 (difference 22%); at x=0.3 the maximum hydrogen mass fraction is 0.095, while on the centre-line it is 0.09 (difference 5%); at x=0.50 m the maximum hydrogen concentration is located on the centre-line.

4. Conclusions

Simulations of the underexpanded plane and round jets of hydrogen were conducted in order to investigate potential to control hydrogen-air mixing and concentration decay in hydrogen jets.

Though the plane nozzle studied had a large aspect ratio L/W=200, the jet behaviour was clearly three- not two-dimensional. The phenomena of "switch" of axes was reproduced by numerical simulations which is characteristic for plane jets with finite aspect ratio. The simulations confirmed that the plane nozzle jet provides faster mixing in the close to the nozzle area, but becomes axisymmetric in the far filed.

It appears that there is practically no quantitative difference between the plane and round nozzle jets from the safety distance point of view. Indeed, hydrogen concentration on the jet axis drops to the low flammability limit of 4% by volume at the same location for both types of jets with the same mass flow rate.

Examination of this simulation results, analysis [20] and experimental data [21] show that while the flame location for a round nozzle jet corresponds to location of hydrogen volume concentration between 8% and 16% in non-reacting jet from the same nozzle, the flame location for a plane jet corresponds to higher hydrogen concentrations in a plane non-reacting jet. This requires further research.

References

1. Schlihting H. Laminare Strahlausebreitung. ZAMM, 1933:13:260-263.
2. Bickley WG. The plane jet. Phil. Mag. 1937: S.7 23 (156):727-731.
3. Schlihting H. Boundary-Layer Theory. New-York: McGraw-Hill; 1979.
4. Chen CJ, Rodi W. Vertical turbulent buoyant jets – review of experimental data. In: Spalding DB, Editor-in-chief. The Science and applications of heat and mass transfer. Pergamon Press; 1980, V.4.
5. Crane LJ, Pack DC. The laminar and turbulent mixing of jets of compressible fluid. Part I Flow far from the orifice. Journal of Fluid Mechanics 1957:2(5):499-455.
6. Maydew RC, Reed JF. Turbulent mixing of compressible axisymmetric jets (in the half region) with quiescent air. Sandia Corp. Res. Rept SC-4764 (March 1963); 1963.
7. Crane LJ, Pack DC. The mixing of a jet of gas with an atmosphere of a different gas at large distances from the orifice. Part I. The plane jet. Quot. Journ. Mech. and Applied Math. 1961:XIV(4):385-391.

8. Schefer R, Houf W, Williams T, Bourne B, Colton J. Characterization of high-pressure, underexpanded hydrogen-jet flames. International Journal of Hydrogen Energy 2007:32:2081 – 2093.
9. Molkov V. Fundamentals of hydrogen safety engineering. In: Teaching materials of the 4th European Summer School on Hydrogen Safety. 7-16 September 2009, Ajaccio, France.
10. Krothapalli A, Baganoff D, Karamcheti K. On the mixing of a rectangular jet. Journal of Fluid Mechanics 1981:107:201-220.
11. Hsia Y, Krothapalli A, Baganoff D, Karamcheti K. The structure of a subsonic compressible rectangular jet. NASA-CR-169110; SU-JIAA-TR-43 (Jan 1, 1982); 1982.
12. Krothapalli A, Hsia Y, Baganoff D, Karamcheti K. On the structure of an underexpanded rectangular jet. NASA-CR-169734; SU-JIAA-TR-47 (Jul 1, 1982); 1982.
13. Gutmark E, Schadow KC, Wilson KJ. Noncircular jet dynamics in supersonic combustion. Journal of Propulsion and Power 1989:5(5):529-533.
14. Gutmark E, Schadow KC, Bicker CJ. Near acoustic field and shock structure of rectangular supersonic jets. AIAA Journal 1990:28(7):1163-1170.
15. Rajakuperan E, Ramaswamy MA.An experimental investigation of underexpanded jets from oval sonic nozzles. Experiments in Fluids 1998:24(4):291-299.
16. Usami M, Niimi S, Imura T, Takahashi T. DSMC calculation of supersonic free jet through a rectangular or a multi-aperture orifice by an improved new collision scheme. Proc. 26th International Symposium “Rarefied Gas Dynamic”. The Institution of Engineering and Technology (ISBN 0094-243X), 2008:1135-1140.
17. Xu H, Zhang J, Wen J, Dembele S, Karwatzki J. Study of a highly under-expanded hydrogen jet. Proc. Int. Conf. on Hydrogen Safety, Pisa, Italy, 8-10 September 2005.
18. Launder BE, Spalding DB. The Numerical computation of turbulent flow. Comp. Meth. Appl. Mech. Eng. 1974:4:269–289.
19. Molkov VV, Bragin MV. High-pressure hydrogen leak through a narrow channel. In: Non-equilibrium Phenomena: Plasma, Combustion, Atmosphere, Moscow, 2009, pp.332-338
20. Molkov VV. Hydrogen safety: state of the art and recent progress. Part II: Hydrogen jet fires. In: 8th Int. Short Course and Advanced research Workshop “Progress in Hydrogen Safety”, 14-18 June 2010, Belfast.
21. Mogi T, Horiguchi S. Experimental study on the hazards of high-pressure hydrogen jet diffusion flames. Journal of Loss Prevention in the Process Industries 2009:22:45-51.